Polariton lasers based on semiconductor quantum microspheres

Pierre Bigenwald,[1] Valentin V. Nikolaev,[2] Dmitry Solnyshkov,[1,2] Alexey Kavokin,[1] Guillaume Malpuech,[1] and Bernard Gil[3]
[1]*LASMEA, CNRS/Université Blaise Pascal Clermont-Ferrand, 24 Avenue des Landais, 63177 Aubière Cedex, France*
[2]*A.F. Ioffe Institute, 26, Polytechnicheskaya, Saint Petersburg, 194021, Russia*
[3]*Group d'Etude de Semiconducteurs, CC 074, Montpellier, France*
(Received 9 June 2004; published 30 November 2004)

We show theoretically that semiconductor microspheres are excellent systems for observation of the polariton lasing and Bose condensation. The strong coupling between bulk exciton states and spherical cavity modes results in the formation of a single exciton-polariton state splitted from the excitonic band. Simulation of polariton relaxation shows that the Bose condensate of exciton polaritons can be formed in this state at pumping intensity of about 1 μW. Spontaneous symmetry breaking in the polariton condensate in the spherical cavity is expected to yield focused emission in some preferential directions that evolve with time.

DOI: 10.1103/PhysRevB.70.205343 PACS number(s): 42.55.Tv, 71.36.+c, 42.50.−p, 71.35.Lk

I. INTRODUCTION

Semiconductor microspheres represent zero-dimensional photonic dots.[1] Their spectrum consists of quantized weakly confined short-living "breathing modes" and strongly confined long-living "whispering gallery modes."[2,3] The difference between them resides in the orbital quantum numbers, either close to 1 (breathing modes) or much larger (whispering gallery modes). Lasing and optical bistability linked to excitonic transitions and exciton-biexciton interplay in the microspheres with or without embedded quantum dots have been reported recently.[4,5] When the optical cavity modes are strongly coupled with excitons, exciton-polariton states appear in the system.[6] Polariton lasing effect[7] consists of the accumulation of exciton-polaritons in one of the discrete quantum states in the system. These accumulated (condensed) polaritons emit a monochromatic and coherent light that has all properties of the laser light. The accumulation is possible due to the bosonic nature of the polaritons evidenced in recent experiments on planar semiconductor microcavities.[8] In this work, we show that the low density of states, discrete spectrum and enhanced light-matter coupling strength make microspheres extremely attractive for the realisation of polariton lasers. These lasers would have an extremely low threshold pumping and may be used as quantum light sources and even single-photon sources, that are of high interest for applications in quantum computing.

We consider here the example of a realistic CdTe bulk microsphere to demonstrate by a numerical simulation a pronounced polariton laser effect at low temperatures. We expect polariton lasing at room temperature be possible in GaN- or ZnO-based microspheres where the exciton oscillator strength is larger.

One can physically distinguish three different light-matter coupling regimes depending on how the size of the sphere R compares with the exciton Bohr radius a_B and wavelength of light at the exciton frequency $\lambda_0 = c/\omega_0$.[9] The first one corresponds to $a_B \approx R \ll \lambda_0$. In this case, free light modes are coupled with excitonic states in spherical quantum dots.[10,11] The exciton energies are quantized because of the quantum confinement, and excitons behave as fermionic electron-holes pairs. Their coupling with light results in radiative broadening of the exciton resonances.

The second regime corresponds to $a_B \ll R \approx \lambda_0$. In this case, the exciton quantization is negligible and excitons behave as bosonic particles. They efficiently couple[12] to quantized optical modes having small angular momenta, relatively small quality factor, and strong splitting between states having different quantum numbers (breathing modes). The light-matter coupling results in formation of short-living exciton-polariton states redshifted with respect to the bare exciton continuum, as we will show below.

Finally, the third regime holds if $a_B \ll \lambda_0 \ll R$. In this case, excitons couple with the whispering gallery modes[2] which are localized at the surface of the sphere. These modes have a very high quality factor and are very close to each other in energy. Light-matter coupling in the latter case results in the formation of long-living mixed modes, involving many photonic states which make the description of the system interesting but rather complicated. Whispering gallery modes are potentially interesting for polariton lasing while their coupling to bulk excitons is reduced with respect to the breathing modes.

In this paper, we concentrate on the intermediate case of the spheres whose size is of the order of the wavelength of light at the exciton resonance. This regime is highly advantageous for exploiting strong light-matter coupling effects and, in particular, for achievement of the polariton lasing. The paper is organized as follows. In Sec. II, we present a calculation of the density of exciton-polariton states and absorption spectrum for a bulk CdTe spherical microcavity (SMC) and demonstrate the strong coupling regime. In Sec. III, we solve the Boltzmann equation to describe the energy relaxation of the exciton-polaritons. We show that, above a threshold pumping, the Bose condensate of polaritons is formed at the lowest energy state, which results in polariton lasing. Section III contains the conclusions on possible application of SMC's in polariton lasers and their potentiality for quantum informatics.

II. LINEAR OPTICAL PROPERTIES OF SPHERICAL MICROCAVITIES

Our model structure represents a SMC having a radius $R = 276.5$ nm: it corresponds to the energy of 1600 meV of

the $1p$-TE optical mode which is resonant with the ground-state exciton energy in CdTe. We assume the cubic phase of the semiconductor that makes the system completely isotropic within the effective mass approximation.

To describe photonic states in a spherical cavity, we use the formalism of Ref. 6 and study both TE and TM polarizations of light. In a dielectric sphere having isotropic and constant permittivity ε and permeability μ, the photon electric and magnetic fields are given by

$$\overrightarrow{H_{l,m}} = a_{\mathrm{TM}}^{l,m} j_l(k_p r)\vec{L}Y_{l,m}(\theta,\varphi), \overrightarrow{E_{l,m}} = \frac{ic}{\varepsilon\omega} a_{\mathrm{TM}}^{l,m}\vec{\nabla}\times[j_l(k_p r)\vec{L}Y_{l,m}(\theta,\varphi)], \quad (1)$$

for the TM-polarized modes and

$$\overrightarrow{E_{l,m}} = a_{\mathrm{TE}}^{l,m} j_l(k_p r)\vec{L}Y_{l,m}(\theta,\varphi), \overrightarrow{H_{l,m}} = \frac{-ic}{\mu\omega} a_{\mathrm{TM}}^{l,m}\vec{\nabla}\times[j_l(k_p r)\vec{L}Y_{l,m}(\theta,\varphi)], \quad (2)$$

for the TE-polarized modes. Here, $j_l(k_p r)$ are the spherical Bessel functions while $Y_{lm}(\theta,\varphi)$ are spherical harmonics indexed by integers l and m, k_p is the eigenvector for the photon state, and (r,θ,φ) are the cylindrical coordinates. The coefficients $a_{\mathrm{TE,TM}}$ ensure the normalization through the integration of the electromagnetic energy density in the cavity:

$$\frac{1}{16\pi}\int_0^R \left(\varepsilon\vec{E}\vec{E}^* + \frac{\vec{H}\vec{H}^*}{\mu}\right) r^2 dr = F\hbar\omega,$$

F is the confinement factor for the considered optical mode and $\vec{L}$ is the differential operator for angular momentum $\vec{L} = (\vec{r}/i)\times\vec{\nabla}$.

In this work, we consider a sphere surrounded by a dielectric environment (glass or vacuum). Therefore, the boundary condition for the photonic mode is that the tangential electric field is maximal for $r=R$. By setting this condition, we obtain numerically series of discrete photon states labeled $1s, 1p, 1d\ldots, 2s, 2p, 2d\ldots$, $ns, np, nd\ldots$. This notation is very different from the atomic one. We no longer have the restriction $n>l$, and the photon "quantum" number n corresponds to the nth values of $k_p R$ that satisfies the boundary condition for a given value of l. The energy hierarchy of states is also different from one adapted to describe the atom but we keep the usual $(2l+1)$ degeneracy for each value of l corresponding to all possible values of m which changes between $-l$ and $+l$. We eliminate any s state from the solution's set since spherical electromagnetic waves having a spherical symmetry cannot exist. Such a wave would have a magnetic field diverging at the center, which is incompatible with Maxwell equations. We focused our study on the $1p$ TE-polarized photonic state. For the sphere size we consider, the closest photon state is $1d$ TM polarized which is separated from the previous one by more than 100 meV.

Concerning the exciton part, we have assumed that the spherical potential well is infinitely deep. The eigenfunctions for such confined states $\Psi_{nlm}(r,\theta,\varphi)$ are decomposed in the product of a spherical Bessel function $j_l(k_x r)$ with the spherical harmonics $Y_{lm}(\theta,\varphi)$, k_x being the eigenvector for the exciton state, (r,θ,φ) are cylindrical coordinates. The exciton energy with respect to the bottom of the well is associated with the kinetic energy of the center of mass and is then given by the formula $E_x=(\hbar k_x)^2/2m_x$, where $m_X=m_e+m_h$.

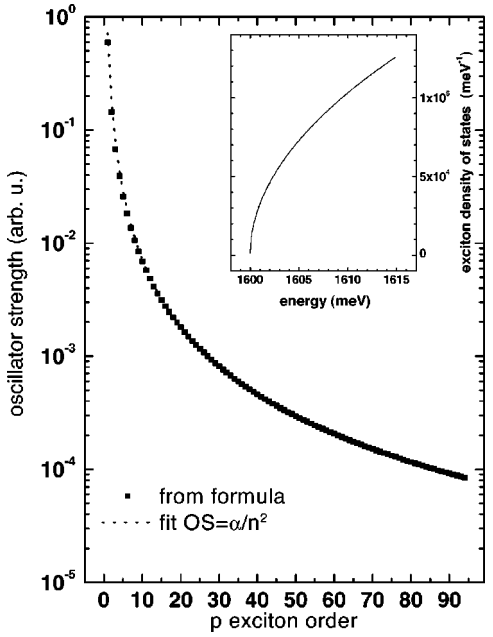

FIG. 1. The oscillator strength of the exciton coupled to a spherical cavity $1p$-TE photon mode calculated with Eq. (5) versus the order of the p exciton state (black squares). The fit by a quadratically decaying function $f(n)=\alpha/n^2$ is shown by a dotted line. The inset displays the exciton density of states dn/dE for the considered CdTe SMC.

In cubic semiconductors the electron and hole masses are isotropic. We also assume them to be independent on the value of k_x. By setting the boundary condition $\Psi_{nlm}(R,\theta,\varphi)=0$, we find a set of solutions similar to one we obtained for the photon mode, the only difference comes from the fact that now the $1s$ configuration corresponds to the exciton ground state. Due to the heavy mass of the exciton, the energy splitting between these states is very small, typically ~ 10 μeV so we have included exciton states up to very large values of $l\sim 90$ and $n\sim 280$ to describe accurately the optical properties of such a SMC over a 25 meV energy range.

The inset to Fig. 1 shows the excitonic density of states dn/dE relation obtained for the considered SMC. It is the same relation as one obtained for the bulk material, $dn/dE = A\sqrt{E-E_0}$, a logical result since the SMC radius R is very large compared to the exciton Bohr radius a_B.

To describe the electric field coupling to the exciton dipole, the most convenient is to work with the Cartesian projections of the electric field. For the TE-polarized wave, we are then able to compute the overlap integral between the electric field and the exciton wave function

$$\vec{I}(1,m,n',l',m') = \int \overrightarrow{E_{l,m}}(\vec{r})\Psi_{n',l',m'}(\vec{r})d^3r, \quad (3)$$

which obeys the following selection rules:

$$\vec{I} = \frac{\delta_{1l'} I' a_{\mathrm{TE}}^{1,m}}{2\sqrt{2}} \begin{pmatrix} \sqrt{(1-m)(2+m)}\,\delta_{m',m+1} + \sqrt{(1+m)(2-m)}\,\delta_{m',m-1} \\ -i\left(\sqrt{(1-m)(2+m)}\,\delta_{m',m+1} - \sqrt{(1+m)(2-m)}\,\delta_{m',m-1}\right) \\ 2m\,\delta_{m',m} \end{pmatrix}. \tag{4}$$

Here I' is the radial part of the integral which is written as $I' = \int_0^R j_1(k_p r) j_1(k_x r) r^2 dr$. These selection rules imply that the only exciton states coupled to the fundamental light mode have $l_{\mathrm{ex}} = 1$, i.e., these are p states. The radial integral can be done analytically:

$$I' = \frac{st\left(\frac{\sin u}{u} + \frac{\sin v}{v}\right) + \cos u - \cos v}{\sqrt{[s(s + \cos s \sin s) - 2\sin^2 s][t(t + \cos t \sin t) - 2\sin^2 t]}}, \tag{5}$$

with the reduced variables $s = k_x R$, $t = k_p R$, $u = s + t$, $v = s - t$.

We will then define the intensity of the light-matter coupling through its oscillator strength f proportional to I^2 which includes the normalization constant of the electric field $|a_{\mathrm{TE}}^{1,m}|^2 = \{32\pi(k_p t)^3/[2t^4 - 2t^2 - 2t\sin(2t) + \cos(2t) - 1]\}(F_{\mathrm{TE}}\hbar\omega/\varepsilon)$. The evolution of f with n, the radial quantum number of the p-exciton wave function, is displayed in Fig. 1 in black squares. It is compared with a quadratically decaying function $f(n) = \alpha/n^2$ shown by a dotted line. The fit is excellent except for the very small values of n where the discrepancies are about a few percent.

We have next calculated the longitudinal-transverse splitting for polariton modes born from the coupling between $1p$ TE-photon and np exciton states. We have used the following formula:

$$\Omega'_{\mathrm{LT}}(\mathrm{SMC}) = I^2 \Omega_{\mathrm{LT}}(\mathrm{bulk})$$

and written the coupling potential as

$$V = \hbar \sqrt{\frac{(1 + 1/R) c \Omega'_{\mathrm{LT}}}{n(R + R')}}, \tag{6}$$

where n is the refraction index of the sphere, and $R' = R$ is the penetration length of the photon in the dielectric environment surrounding the sphere. We associate to each coupled mode's eigenenergy an imaginary part reflecting its lifetime in the cavity: we take $\gamma = 0.05$ meV for the excitons and $\Gamma = 0.2$ meV for the optical mode which corresponds to a 3 ps lifetime.[13] The polariton eigenenergies are eigenvalues of the energy matrix of the coupled states $(1p_p, 1p_x, \ldots, np_x)$, once again displaying a real part E and an imaginary part G. These states can have three different values of the angular momentum ($m = -1$, 0, $+1$) and are therefore three-fold degenerated. The fundamental photon mode E_{p0} may be detuned from the exciton fundamental mode E_{x0} by δE for which we chose three different values: 0, -10, or $+10$ meV.

Figure 2 shows the microsphere polariton density of state $dn(E)/dE$ resulting from the coupling between excitons and the photon mode for three abovementioned values of the detuning. We have assumed the bare exciton ground state has an energy of 1600 meV. One can observe for all detunings the appearance of a fundamental exciton-polariton eigenstate, further referred to as lower polariton state (LPS). It is located well below the bare exciton and photon energy. The photon part of the LPS depends on the detuning δE, the 50/50 exciton-photon share appears for $\delta E \sim 10$ meV which corresponds to equal magnitudes of LPS and upper-polariton state (UPS) peaks. The coupling also results in the formation of an upper polariton band (UPB) that is degenerated with the exciton continuum and does not appear on the density of state. One should note that, apart from the formation of two new mixed modes, exciton states remains essentially unperturbed and do not gain any significant photon fraction from the coupling. Figure 3 shows the calculated absorption coefficient $\alpha(E)$ given by $\alpha(E) = x_L(E) G(E)[dn(E)/dE]$ where x_L is the photon fraction of a polariton mode.

In the absorption spectrum one can well see the upper polariton states which show their partly photonic nature. They are however broadened due to their degeneracy with the bare exciton continuum. One can also observe the appearance of a small absorption peak at 1600 meV common to three curves. Its intensity is maximal for $\delta E = 0$. This shows that not only two, but at least a few exciton states start

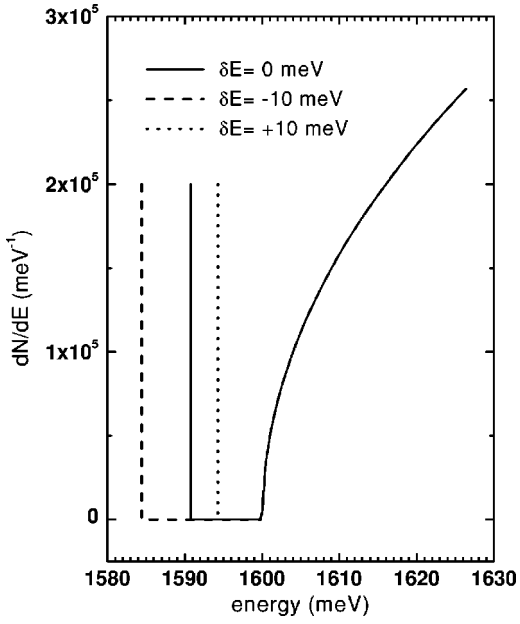

FIG. 2. Calculated exciton density of states versus the energy for a CdTe spherical microcavity for different values of the energy detuning between exciton and photon fundamental states. Above $E_0 \sim 1.6$ eV, the three curves merge and follow the bulk density of states: $dN/dE = A\sqrt{E - E_0}$.

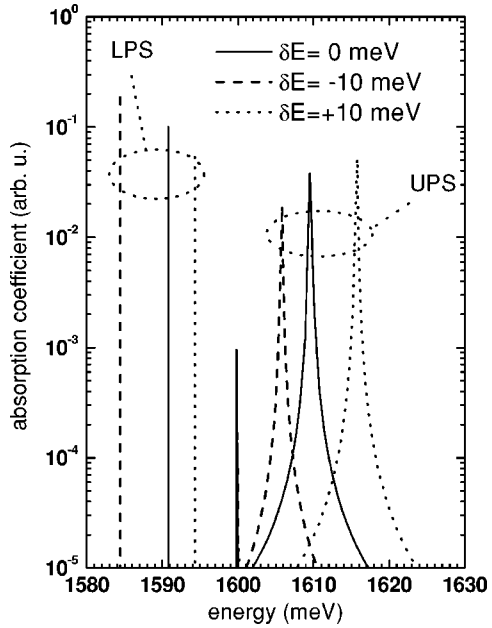

FIG. 3. Calculated absorption coefficient versus the energy for a CdTe spherical microcavity for different values of detuning between the exciton resonance frequency and 1*p*-TE photon mode. Detuning between the photon and exciton energies induces a modification of the photonic part between upper polariton state (UPS) and lower polariton state (LPS): at positive detuning $\delta E \sim 10$ meV the 50/50 balance between these states is achieved. Three curves display a common peak at $E_0 = 1600$ meV which intensity is maximal for $\delta E = 0$.

having a nonzero photonic fraction as a result of coupling to the cavity mode.

III. NONLINEAR OPTICAL PROPERTIES OF SPHERICAL MICROCAVITIES

In order to show the advantage of the peculiar density of polariton states obtained in Sec. II, we have performed a simulation of the exciton-polariton relaxation dynamics in this structure. The method is based on the resolution of the semiclassical Boltzmann equation describing boson relaxation (see Ref. 7, Chap. 4):

$$\frac{dN_i}{dt} = P_i - \frac{N_i}{\tau_i} + (N_i + 1)\sum_{j \neq i} W_{j \to i} N_j - N_i \sum_{j \neq i} W_{i \to j}(N_j + 1), \tag{7}$$

where N_i is the population of the state i, P_i is the eventual external pumping of the state i, τ_i is the lifetime of the state i given by the imaginary part of its energy, and $W_{i \to j}$ are the scattering rates from the state i to the state j. Excitons, or electron-hole pairs can be introduced in the system by electrical or optical pumping nonresonantly. An alternative efficient way to introduce noncoherent excitons in the system is to resonantly pump the upper polariton mode from where polariton quickly relax to the exciton continuum. We have considered this latter configuration which has the advantage of injecting to the system the excitons possessing the same angular quantum numbers as the lower polariton mode. We have taken into account the exciton-exciton and exciton-acoustic phonon scattering. In a system with the spherical symmetry, elastic scattering does not involve wave-vector conservation, but only requires quantum number and energy conservation.

Scattering rates from a state 1 to a state 2, having energies E_1 and E_2, respectively, coming from exciton-exciton interaction read

$$W_{1,2}^{xx} = \frac{2\pi}{\hbar}|M_x|^2 \int x_1 x_3 \frac{dn}{dE}(E_1 - E_2 + E_3)\frac{dn}{dE}(E_3) N_x(E_3) \times [1 + N_x(E_1 - E_2 + E_3)] dE_3, \tag{8}$$

where E_3 is the initial energy of the "second" polariton, which participates in the scattering act, x_1 and x_3 are excitonic fractions of the corresponding polaritons, M_x is the average matrix element of the exciton-exciton interaction, and $dn(E)/dE$ denotes the density of states. We use the matrix element of bulk exciton interaction $M_x = E_B (a_B)^3 / V$, where V is the volume of the sphere.

The interaction with acoustic phonons has been calculated using the following approximations. The phonons were considered to be bulklike, three dimensional, and freely propagating, the matrix element of exciton-phonon interaction was taken as

$$|M_{\mathrm{ph}}|^2 = \frac{D^2 E}{\hbar \rho c^2 V}\left(1 + \frac{m_e a_B E}{2\hbar(m_e + m_h)}\right)^{-2}, \tag{9}$$

where c is the speed of sound,[14] ρ is the density, and D is the deformation potential of CdTe.[15]

The density of states for bulk acoustic phonons in the Debye approximation is

$$\frac{dn_{\mathrm{ph}}(E)}{dE} = \frac{VE^2}{(2\pi)^2(\hbar c)^3}. \tag{10}$$

Using these expressions, we can write the scattering rate for polariton interaction with acoustic phonons as

$$W_{1,2}^{\mathrm{ph}} = \frac{2\pi}{\hbar}|M_{\mathrm{ph}}|^2 x_1 \left\{ \begin{array}{c} \frac{dn_{\mathrm{ph}}}{dE}(E_2 - E_1) n_{\mathrm{ph}}(E_2 - E_1) \\ \frac{dn_{\mathrm{ph}}}{dE}(E_1 - E_2)(1 + n_{\mathrm{ph}}(E_1 - E_2)) \end{array} \right\}, \tag{11}$$

where the top line corresponds to absorption of phonons, and the bottom line corresponds to phonon emission. We have also considered the dynamical blue shift of the polariton states energy induced by the polariton-polariton interaction. This shift can estimated in the framework of the Bogoliubov approximation as

$$E_i(t) = E_i(0) + |M_x|^2 N_i^2, \tag{12}$$

where I is the index of the state.

We have adapted the following initial conditions: at negative times the structure is empty, at $t = 0$ the pumping is switched on. We solve numerically Eq. (7) until the system reaches its steady state. Figure 4 shows, for two different

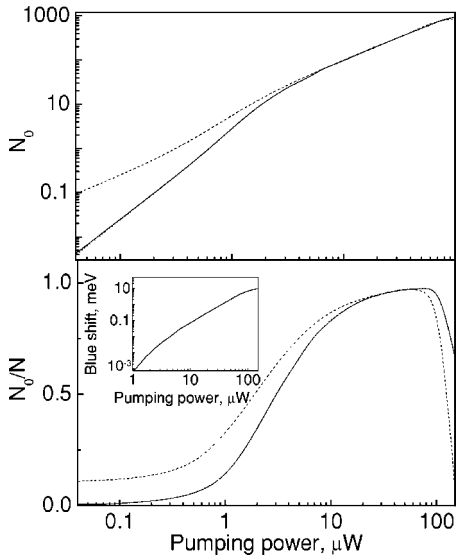

FIG. 4. (a) Calculated number of particles in the ground polariton state (N_0) versus pumping power. (b) Fraction of particles in the ground state N_0/N and the blueshift (inset) versus pumping power: for zero detuning (solid line), +10 meV detuning (dashed line).

detunings, the number of particles in the ground state N_0 as a function the pumping power as well as the fraction of particles in the ground state N_0/N in the steady state regime. The plot of N_0 is in the logarithmic scale where the slope of curves indicates the dependence of N_0 on pumping. For zero detuning, N_0 grows quadratically with the pumping power below the stimulation threshold which indicates that the relaxation toward the ground state is governed by the polariton-polariton interaction. For positive detuning, N_0 grows linearly which indicates that polariton relaxation down to the ground state is dominated by phonon scattering. A stimulation threshold takes place for a pumping power of about 1 μW. It is marked by a change in the slope of the curve which corresponds to the exponential increase of N_0. It takes place when the number of particles within the ground state achieves one. In this regime, the ground-state fraction rapidly increases and almost all the particles are accumulated in the ground state. Above 80 μW, the fourth regime takes place. The ground-state population becomes so large ($\sim$1000) that a significant blueshift of the ground-state energy takes place due to the polariton-polariton interaction as the inset to Fig. 4 shows. When this shift becomes comparable to the Rabi splitting, the polariton state becomes degenerated with the exciton continuum. The ground-state population ceases to increase with pumping intensity and the ground state fraction rapidly drops. We also want to point out that the total maximum polariton density achieved is about 10^{16} cm^{-3}, i.e., orders of magnitude below the exciton bleaching density.

IV. CONCLUSIONS

We have shown that exciton-light coupling in submicron semiconductor microspheres can lead to the formation of an exciton-polariton state red shifted with respect to the exciton absorption edge. When the microsphere is optically pumped, the relaxation toward the ground state is enhanced by bosonic stimulated scattering and polariton lasing takes place with an extremely small threshold (1 μW). The emission pattern of the TE $1p$ mode has *a priori* some well defined angular features. However, in the spontaneous relaxation regime, ground-state polaritons have a random phase and their total emission should have a complete spherical symmetry. The situation dramatically changes above the stimulation threshold. In this regime, a spontaneous symmetry breaking effect takes place and results in the locking of the emission pattern along well-defined axes (pinning of the $1p$ mode). The switching from a spherical emission pattern to a directional one with increasing pumping intensity could therefore be interpreted as an evidence for exciton-polariton Bose condensation. Moreover, the emission patterns of $m=1$ and $m=0$ polariton states are not identical. Two beams corresponding to these two different quantum numbers can be quantum-mechanically correlated because of the polariton-polariton interaction. Quantum correlations between spatially separated monochromatic emission patterns could give rise to formation of so-called Einstein-Podolsky-Rosen pairs[16] which are of high interest for quantum computing applications. In the present work we did not consider quantum correlations between $m=1$ and $m=0$ polaritons. Investigations aimed at description of quantum effects in emission of spherical microcavities would require going beyond the Boltzmann equations. We foresee new discoveries on this way.

[1] K.J. Vahala, Nature (London) **424**, 6950 (2003); L. Banyai, S.W. Koch, Phys. Rev. Lett. **57**, 2722 (1986).
[2] A.N. Oraevsky, M.O. Scully, T.V. Sarkisyan, and D.K. Bandy, Laser Phys. **9**, 990 (1999).
[3] U. Woggon, R. Wannemacher, M.V. Artemyev, B. Moller, N. Lethomas, V. Anikeyev, and O. Schops, Appl. Phys. B: Lasers Opt. **77**, 469 (2003).
[4] M. Nagai, F. Hoshino, S. Yamamoto, R. Shimano, and M. Kuwata Gonokami, Opt. Lett. **22**, 1630 (1997).
[5] S.L. Lu, R. Jia, D.S. Jiang, and S.S. Li, Physica E (Amsterdam) **17**, 453 (2003).
[6] M.A. Kaliteevski, S. Brand, R. Abram, V.V. Nikolaev, M.V. Maximov, C.M. Sotomayor-Torres, and A.V. Kavokin, Phys. Rev. B **64**, 115305 (2001).
[7] A. Kavokin and G. Malpuech, *Cavity Polaritons* (Elsevier, Amsterdam, 2003).
[8] L.S. Dang, D. Heger, R. Andre, F. Boeuf, and R. Romestain, Phys. Rev. Lett. **81**, 3920 (1998); P.G. Savvidis, J.J. Baumberg, R. M. Stevenson, M.S. Skolnick, D.M. Whittaker, and J.S. Roberts, *ibid.* **84**, 1547 (2000); H. Deng, G. Weihs, C. Santori, J.

Bloch, and Y. Yamamoto, Science **298**, 199 (2002).
[9] J.R. Buck and H.J. Kimble, Phys. Rev. A **67**, 033806 (2003).
[10] R. Ferreira, O. Verzelen, and G. Bastard, Physica E (Amsterdam) **21**, 164 (2004).
[11] H. Ajiki, T. Tsuji, K. Kawano, and K. Cho, Phys. Rev. B **66**, 245322 (2002).
[12] B. Gil and A. Kavokin, Appl. Phys. Lett. **81**, 748 (2002).
[13] G. Vijaya Prakash, L. Besombes, T. Kelf, J.J. Baumberg, P.N. Bartlett, and M.E. Abdelsalam, Opt. Lett. (to be published).
[14] M.H. Krisch, A. Mermet, A. San Miguel, F. Sette, C. Masciovecchio, G. Ruocco, and R. Verbeni, Phys. Rev. B **56**, 8691 (1997).
[15] D.J. Dunstan, B. Gil, and K.P. Homewood, Phys. Rev. B **38**, 7862 (1988).
[16] G. Weihs, T. Jennewein, C. Simon, H. Weinfurter, and A. Zeilinger, Phys. Rev. Lett. **81**, 5039 (1998); C. Simon, G. Weihs, and A. Zeilinger, *ibid.* **84**, 2993 (2000).